CHEMIJA
2026. Vol. 37. No. 1. P. 29–42

ISSN 0235-7216 eISSN 2424-4538
DOI: https://doi.org/10.6001/chemija.2026.37.1.4

Design of ortho/meta-substituted selective carbonic anhydrase IX inhibitors

Mantas Žvirblis,

Vaida Paketurytė-Latvė,

Marius Gedgaudas,

Darius Lingė,

Ernestas Urniežius,

Tautvydas Kojis,

Laimonas Stančaitis,

Audrius Zakšauskas,

Aurelija Mickevičiūtė,

Jelena Jachno,

Vaida Juozapaitienė,

Virginija Dudutienė,

Asta Zubrienė,

Daumantas Matulis*

Department of Biothermodynamics and Drug Design,
Institute of Biotechnology,
Life Sciences Center,
Vilnius University,
7 Saulėtekio Avenue,
10257 Vilnius, Lithuania

In the search for chemical compounds that strongly and selectively bind and inhibit one out of 12 catalytically active CA isozymes, a series of fluorinated substituted benzenesulfonamides was designed and synthesised. Substituents were intended to be stiff and have a limited conformational flexibility. We determined compound affinities using the fluorescence-based thermal shift assay. Afterward, we subtracted the binding-linked protonation reactions and calculated the intrinsic affinities, which were then used to establish the structure–affinity relationships. Compound **5** (2-(cyclohexylamino)-3,5,6-trifluoro-4-(phenylsulfonyl) benzenesulfonamide) exhibited an improved selectivity profile toward CAIX, a cancer-associated isozyme. The analysis of compound functional group contributions and the comparison with previously designed compounds provided insight toward a deeper understanding of the protein–ligand recognition principles for drug design.

Keywords: protein–ligand binding, binding thermodynamics, recombinant proteins, drug design and synthesis, enzyme inhibition, carbonic anhydrase

INTRODUCTION

Drug design relies on the search for small molecules that exert an effect on the target protein or other biomolecule that is responsible for the disease or a specific physiological condition [1]. Despite great methodological developments in the field, the annual introduction of NCEs (new chemical entities) into therapy has decreased from nearly 100 compounds in the 1960s to fewer than 50 in the last several decades.

Why is it so difficult to design chemical compounds that would strongly interact with the target protein but weakly interact with undesired

* Corresponding author. Email: daumantas.matulis@bti.vu.lt

proteins? The high affinity determines the targeted action, while the high selectivity ensures that the new compound would not bind and interfere with proteins whose actions are vital and consequently exhibit a low toxicity. The main reason for the difficulties in the drug design field is a relatively limited understanding of the principles of recognition between a small-molecule chemical compound and a protein molecule. Continuous development of computational models, especially quantum mechanics-based models, is necessary for a detailed prediction of protein–ligand binding affinities [2].

In the search for high-affinity ligands, we have focused on the human carbonic anhydrase (CA) enzyme family. These enzymes have Zn(II) in the active site that binds the primary sulfonamide compounds with a coordination bond, and thus all compounds that possess the sulfonamide group are likely to bind to the CA enzymes, making it easier to study the structure–activity relationship of a series of compounds that all possess the sulfonamide group and bind the enzyme with a measurable affinity. We have synthesised over 700 sulfonamide compounds and determined their affinities to each human CA isozyme, revealing some rules in the design of high-affinity compounds that would selectively recognise only a single target protein. The data have been assembled in the Protein-Ligand Binding Database (PLBD.org) and made available for the application of AI principles for the rational drug design [3].

The human carbonic anhydrase family comprises 15 highly homologous and structurally closely related proteins, among which three isoforms do not possess Zn(II) and thus do not have catalytic activity. The remaining 12 are isozymes possessing the catalytic activity of carbon dioxide hydration into a bicarbonate anion and an acid proton. Thus, CA isozymes participate in numerous physiological processes, such as pH regulation, carbon metabolism, and carbon dioxide gas exchange. Their inhibitors have been shown to exhibit beneficial therapeutic effects in numerous illnesses. The ninth isozyme, CAIX, is highly overexpressed in numerous solid hypoxic tumours, helping cancer spread by acidifying the tumour cell microenvironment, alleviating the invasiveness and metastasis processes, and thus its inhibition is postulated and shown in animal models to be beneficial in cancer treatment [4].

A large number of compounds have been shown to be CA inhibitors [5–7]. However, most compounds bind in the micromolar to nanomolar affinity range. Picomolar binders are relatively rare. We have discovered fluorinated substituted benzenesulfonamide compounds that exhibited picomolar affinities for CAIX [8]. The affinities have been further increased by modifying the compound [9] and especially by introducing a covalent-binding targeted chemical group that may irreversibly inhibit the enzyme [10]. Here we introduce several new inhibitors and perform their structure–activity relationship analysis [11] by comparing functional group contributions to the affinity for human CA isozymes.

MATERIALS AND METHODS

Synthesis and characterisation of compounds

During the synthesis, all starting materials and reagents were commercial products, used without further purification. Column chromatography was performed using Silica gel 60 (0.040–0.063 mm, Merck). ^{1}H and ^{13}C NMR spectra were recorded on a Bruker Ascend 400 spectrometer (400 and 100 MHz, respectively) with TMS as an internal standard, and proton and carbon chemical shifts were expressed in parts per million (ppm) in the indicated solvent. The ^{19}F NMR spectra were recorded on a Bruker Ascend 400 spectrometer (376 MHz) with $CFCl_3$ as an internal standard, and fluorine chemical shifts were expressed in parts per million (ppm) in the indicated solvent. Multiplicity in the spectra was defined as s (singlet), d (doublet), t (triplet), q (quartet), dd (doublet of doublets), ddd (doublet of doublet of doublets), m (multiplet), br s (broad singlet) and dm (double multiplet). Thin-layer chromatography (TLC) was performed with silica gel 60 F254 aluminum plates (Merck) and visualised with UV light. High-resolution mass spectra (HRMS) were recorded by Agilent TOF 6230 equipped with Agilent Infinity 1260 HPLC, in the positive or negative electrospray ionisation (ESI) mode. In the positive mode, the isocratic elution of aqueous acetonitrile solution (95:5, v/v) of 1% formic acid solution (18.2 MΩ·cm at 25°C) was used, in the negative mode acetonitrile and water (80:20, v/v) was used at a flow rate of 0.3–0.5 mL/min.

6,7-difluoro-8-(phenylsulfonyl)-1,2,3,4-tetrahydroquinoxaline-5-sulfonamide (*MZ24-18*, 2)

The mixture of pentafluorobenzenesulfonamide (0.050 g, 0.2 mmol), sodium benzenesulfinate (0.063 g, 0.38 mmol, 1.45 equiv) and 2 mL DMSO was heated at 70°C for 26 h. Then ethylenediamine dihydrochloride (0.027 g, 0.20 mmol, 1 equiv) and Et_3N (113 µL, 3 equiv) were added to the mixture, which was heated again at 70°C for 27 h. The mixture was diluted with 40 mL of H_2O and extracted with EtOAc (10 mL × 3). The extract was dried over $MgSO_4$ and concentrated under reduced pressure. The resulting dark yellow oil was subjected to column chromatography (silica gel, hexane/EtOAc, 1:1, R_f = 0.4), yielding a crystalline material.

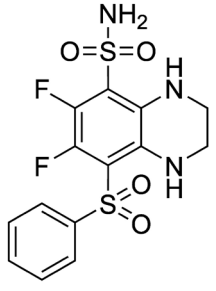

Yield: 0.018 g (23%).

^{1}H NMR (400 MHz, DMSO-d_6, δ): 3.37–3.44 (2H, m, NHC**H**$_2$), 3.45–3.50 (2H, m, NHC**H**$_2$), 7.10 (1H, s, N**H**CH$_2$), 7.62 (1H, s, N**H**CH$_2$), 7.73 (2H, t, *J* = 7.8 Hz, ArH), 7.83 (1H, t, *J* = 7.4 Hz, ArH), 7.93 (2H, s, SO_2NH_2), 8.06 (2H, d, *J* = 7.8 Hz, ArH). **^{13}C NMR** (100 MHz, DMSO-d_6, δ): 38.53 (NHCH$_2$), 39.25 (NHCH$_2$), 108.97 (**C5**, d, $^2J_{CF}$ = 13.27 Hz), 115.33 (**C8**, d, $^2J_{CF}$ = 13.2 Hz), 126.82 (Ar, d, $^4J_{CF}$ = 2 Hz), 130.44 (Ar), 130.91 (C-NH), 133.23 (C-NH), 134.83 (ArH), 137.44 (**C6** or **C7**, dd, $^1J_{CF}$ = 254 Hz, $^2J_{CF}$ = 15.2 Hz), 137.48 (**C6** or **C7**, d, $^1J_{CF}$ = 223 Hz). **^{19}F NMR** (376 MHz, DMSO-d_6, δ): –153.94 (1F, d, $^1J_{FF}$ = 27.9 Hz), –154.27 (1F, d, $^1J_{FF}$ = 27.2 Hz). HRMS $C_{14}H_{14}F_2N_3O_4S_2$ [(M+H)$^+$]: calcd. 390.0388, found 390.0384.

2-(benzylamino)-3,4,5,6-tetrafluorobenzenesulfonamide (*MZ24-21*, 3)

The mixture of pentafluorobenzenesulfonamide (0.150 g, 0.60 mmol), benzylamine (87 µL, 0.78 mmol, 1.3 equiv), triethylamine (85 µL, 0.60 mmol, 1 equiv) and 10 mL toluene was heated at 110°C for 2 h. The mixture was evaporated under reduced pressure. The resulting dark yellow slurry was subjected to column chromatography (silica gel, DCM/EtOAc, 30:1, R_f = 0.42), yielding a white crystalline material.

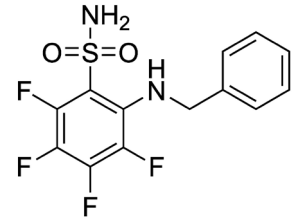

Yield: 0.078 g (38%).

^{1}H NMR (400 MHz, DMSO-d_6, δ): 4.49–4.58 (2H, m, NHC**H**$_2$), 6.95–7.02 (1H, m, N**H**CH$_2$), 7.22–7.42 (5H, m, ArH), 8.23 (2H, s, SO_2NH_2). **^{13}C NMR** (100 MHz, DMSO-d_6, δ): 49.79 (NHCH, d, *J* (^{19}F-^{13}C) = 11.4 Hz), 114.40 (**C2**, d, $^2J_{CF}$ = 13.4 Hz), 127.68 (Ar), 127.74 (Ar), 129.02 (Ar), 131.87 (**C3**, dm, $^1J_{CF}$ = 240.1 Hz), 133.31–133.54 (**C1**, m), 137.85 (**C5**, ddd, $^1J_{CF}$ = 244.4 Hz, $^2J_{CF}$ = 12.7 Hz, $^3J_{CF}$ = 4.0 Hz), 139.60 (Ar, d, $^4J_{CF}$ = 1.8 Hz), 143.52 (**C6**, dm, $^1J_{CF}$ = 250 Hz), 145.65 (**C4**, dm, $^1J_{CF}$ = 250 Hz).

^{19}F NMR (376 MHz, DMSO-d_6, δ): –136.70 (1F, td, $^1J_{FF}$ = 27.9 Hz, $^2J_{FF}$ = 7.2 Hz), –151.91 (1F, td, $^1J_{FF}$ = 21.8 Hz, $^2J_{FF}$ = 6.8 Hz), –154.40; –154.62 (1F, m), –154.27 (1F, ddd, $^1J_{FF}$ = 25.9 Hz, $^2J_{FF}$ = 23.2 Hz, $^3J_{FF}$ = 5.4 Hz).

HRMS $C_{13}H_{11}F_4N_2O_2S$ [(M+H)$^+$]: calcd. 335.0472, found 335.0473.

2-(benzylamino)-3,5,6-trifluoro-4-(phenylsulfonyl) benzenesulfonamide (*MZ24-24*, 4)

The mixture of 2-(benzylamino)-3,4,5,6-tetrafluorobenzenesulfonamide (0.057 g, 0.17 mmol), sodium benzenesulfinate (0.037 g, 0.22 mmol, 1.3 equiv) and 2 mL DMSO was heated at 70°C for 19 h. The mixture was diluted with 30 mL of H_2O and extracted with EtOAc (10 mL × 3). The extract was dried over $MgSO_4$ and concentrated under reduced pressure. The resulting dark yellow oil was subjected to column chromatography (silica gel, Hexane/EtOAc, 3:1, R_f = 0.24) resulting in a pale yellow crystalline material.

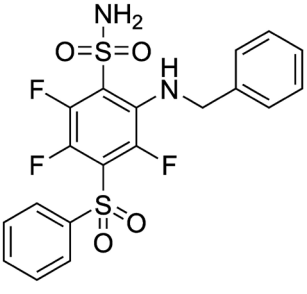

Yield: 0.026 g (33%).

^{1}H NMR (400 MHz, DMSO-d_6, δ): 4.46 (2H, dd, ^1J = 6.5 Hz, ^2J = 4.2 Hz, NHC**H**$_2$), 6.84–6.90 (1H, m, N**H**CH$_2$), 7.19–7.31 (5H, m, CH$_2$Ar**H**), 7.66–7.73 (2H, m, ArH), 7.81–7.87 (1H, m, ArH), 7.97 (2H, d, J = 7.3 Hz, ArH), 8.35 (2H, s, SO$_2$NH$_2$). **^{13}C NMR** (100 MHz, DMSO-d_6, δ): 50.09 (NHCH$_2$, d, $^3J_{CF}$ = 12.7 Hz), 122.64 (**C1**, dd, $^2J_{CF}$ = 17.1 Hz, $^3J_{CF}$ = 12.7 Hz), 123.84 (**C4**, dd, $^2J_{CF}$ = 12.1 Hz, $^3J_{CF}$ = 5.5 Hz), 127.75 (Ar), 127.91, 130.40 (Ar), 133.77 (**C2**, dd, $^2J_{CF}$ = 13.2 Hz, $^3J_{CF}$ = 2.5 Hz), 135.59 (Ar), 138.11 (**C5** or **C6**, ddd, $^1J_{CF}$ = 252.1 Hz, $^2J_{CF}$ = 17.4 Hz, $^3J_{CF}$ = 4.6 Hz), 139.18 (Ar), 144.8 (**C3**, d, $^1J_{CF}$ = 255 Hz), 145.06 (**C5** or **C6**, ddd, $^1J_{CF}$ = 251.7 Hz, $^2J_{CF}$ = 15.7 Hz, $^3J_{CF}$ = 4 Hz). **^{19}F NMR** (376 MHz, DMSO-d_6, δ): –153.94 (1F, d, $^1J_{FF}$ = 27.9 Hz), –154.27 (1F, d, $^1J_{FF}$ = 27.2 Hz).

HRMS $C_{19}H_{16}F_3N_2O_4S_2$ [(M+H)$^+$]: calcd. 457.0498, found 457.0508.

2-(cyclohexylamino)-3,5,6-trifluoro-4-(phenylsulfonyl)benzenesulfonamide (*MZ24-3*, 5)

The mixture of pentafluorobenzenesulfonamide (0.296 g, 1.2 mmol), cyclohexylamine (167 µL, 1.4 mmol, 1.2 equiv), triethylamine (185 µL, 1.3 mmol, 1.1 equiv) and 8 mL of toluene was heated at 110°C for 2 h. The mixture was evaporated under reduced pressure, the resulting thick oil was dissolved in 4 mL of DMSO, and sodium benzenesulfinate (0.297 g, 1.8 mmol, 1.5 equiv) was added. The mixture was heated at 70°C for 24 h, then it was diluted with 40 mL of H_2O and extracted with EtOAc (10 mL × 3). The extract was dried over $MgSO_4$ and concentrated under reduced pressure. The resulting dark yellow oil was subjected to column chromatography (silica gel, Hexane/EtOAc, 3:1, R_f = 0.16), resulting in a pale yellow crystalline material.

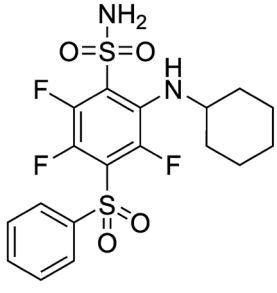

Yield: 0.084 g (15%).

^{1}H NMR (400 MHz, DMSO-d_6, δ): 1.05–1.31 (5H, m, cyclohexane), 1.46–1.55 (1H, m, cyclohexane), 1.58–1.67 (2H, m, cyclohexane), 1.71–1.81 (2H, m, cyclohexane), 3.39 (1H, br. s, NHC**H**), 6.34 (1H, d, J = 8.4 Hz, NH), 7.71 (2H, t, J = 7.8 Hz, ArH), 7.83 (1H, t, J = 7.5 Hz, ArH), 8.04 (2H, d, J = 7.9 Hz, ArH), 8.34 (2H, s, SO$_2$NH$_2$). **^{13}C NMR** (100 MHz, DMSO-d_6, δ): 24.29 (cyclohexane), 25.24 (cyclohexane), 33.66 (cyclohexane), 54.33 (NHCH$_2$, d, $^4J_{CF}$ = 11 Hz), 122.75 (**C1**, dd, $^2J_{CF}$ = 17.1 Hz, $^2J_{CF}$ = 12.7 Hz), 123.50 (**C4**, dd, $^2J_{CF}$ = 12.1 Hz, $^2J_{CF}$ = 5.5 Hz), 127.82 (Ar), 130.38 (Ar), 133.22 (**C2**, dd, $^2J_{CF}$ = 13.4 Hz, $^3J_{CF}$ = 2.8 Hz), 135.57 (Ar), 138.17 (**C5** or **C6**, ddd, $^1J_{CF}$ = 251.3 Hz, $^2J_{CF}$ = 17.8 Hz, $^3J_{CF}$ = 4.6 Hz), 140.90 (Ar), 144.98 (**C3**, d, $^1J_{CF}$ = 256.8 Hz), 145.26 (**C5** or **C6**, ddd, $^1J_{CF}$ = 253.6 Hz, $^2J_{CF}$ = 15.8 Hz, $^3J_{CF}$ = 4.2 Hz). **^{19}F NMR** (376 MHz, DMSO-d_6, δ): –124.10; –124.18 (1F, m), –134.47 (1F, dd, $^1J_{FF}$ = 27.2 Hz, $^2J_{FF}$ = 12.3 Hz), –150.41 (1F, dd, $^1J_{FF}$ = 26.6 Hz, $^2J_{FF}$ = 8.9 Hz).

HRMS $C_{20}H_{20}F_3N_2O_4S_2$ [(M+H)$^+$]: calcd. 449.0811, found 449.0812.

2,3-difluoro-4-((2-hydroxyethyl)sulfonyl)-5,5a,6,7,8,9,9a,10-octahydrophenazine-1-sulfonamide (*MZ24-46*, 7)

The mixture of 2,3,5,6-tetrafluoro-4-((2-hydroxyethyl)sulfonyl) benzenesulfonamide[12] (0.062 g, 0.18 mmol), cis-cyclohexane-1,2-diamine (0.023 g, 0.2 mmol, 1.1 equiv), triethylamine (51 µL, 0.36 mmol, 2 equiv) and 2 mL DMSO was heated at 70°C for five days. The mixture was diluted with 20 mL of H_2O and extracted with EtOAc (10 mL × 3). The extract was dried over $MgSO_4$ and concentrated under reduced pressure. The resulting dark yellow oil was subjected to gradient column chromatography (silica gel, Hexane/EtOAc, 1:1 to 2:1, R_f = 0.4 (2:1, Hexane:EtOAc)), yielding pale yellow crystals.

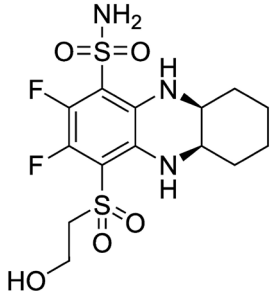

Yield: 0.019 g (25%).

^{1}H NMR (400 MHz, DMSO-d_6, δ): 1.26–1.38 (2H, m, cyclohexane), 1.44–1.72 (6H, m, cyclohexane),

3.45–3.58 (4H, m, CH_2SO_2), 3.74–3.83 (2H, m, C**H**$_2$OH), 4.94 (1H, br. s., OH), 6.90 (1H, s, NH), 7.18 (1H, s, NH), 7.95 (2H, s, SO_2NH_2). ^{13}**C NMR** (100 MHz, DMSO-d_6, δ): 21.73 (cyclohexane), 21.90 (cyclohexane) 29.90 (cyclohexane), 47.38 (cyclohexane), 47.74 (cyclohexane), 55.45 (SO_2CH_2), 59.57 (CH_2OH), 108.37 (**C1**, d, $^2J_{CF}$ = 13.2 Hz), 115.20 (**C4**, d, $^2J_{CF}$ = 12.8 Hz), 129.95 (C-NH), 132.99 (C-NH), 137.60 (**C2** or **C3**, dd, $^1J_{CF}$ = 243.2 Hz, $^2J_{CF}$ = 20.9 Hz), 138.29 (**C2** or **C3**, dd, $^1J_{CF}$ = 243.2 Hz, $^2J_{CF}$ = 20.9 Hz). ^{19}**F NMR** (376 MHz, DMSO-d_6, δ): –154.13 (1F, d, $^1J_{FF}$ = 27.3 Hz), –154.30 (1F, d, $^1J_{FF}$ = 27.3 Hz).

HRMS $C_{14}H_{20}F_2N_3O_5S_2$ [$(M+H)^+$]: calcd. 412.0807, found 412.0810.

Preparation of recombinant CA isozymes

Among 15 human CA isoforms, there are 12 catalytically active human CA isozymes, which were prepared recombinantly as previously described. Most isozymes were truncated, and only the catalytic domains of the proteins were produced [8, 13]. All isozymes were expressed in the bacterial expression system, except CAVI and CAIX, which were expressed in mammalian cells. The proteins were chromatographically purified via IMAC, ion-exchange, or p-aminomethylbenzene sulfonamide-sepharose affinity chromatography. The SDS-PAGE of each protein preparation was performed to show the approximate protein MW and the absence of unknown protein impurities. Precise MW was determined by mass spectrometry with 1 Da precision, and it matched the value calculated from the protein amino acid sequence.

Fluorescent thermal shift assay

The fluorescence-based thermal shift assay (FTSA) was used to determine the binding affinity of compounds for selected catalytically active CA isozymes. During the assay, the protein solution is heated, and the melting temperature T_m is determined. Small-molecule binding ligands usually stabilise the proteins, and the assay distinguishes itself in its ability to determine an extremely high affinity (picomolar K_d) of compound binding to CA. The experiments were performed using a QIAGEN Rotor-Gene Q instrument using the blue channel (365 ± 20 nm excitation and 460 ± 15 nm emission detection) or the green channel (470 ± 10 nm excitation and 510 ± 5 nm detection). The protein solution, in the absence and presence of various compound concentrations ranging from 3 to 200 μM (2x dilutions), was heated from 25 to 99°C (heating rate 1°C/min). The CA isozyme T_m was determined by following the fluorescence of 8-anilino-1-naphthalene sulfonate (ANS) or Glomelt™ dye. The samples consisted of 5 μM protein (or 10 μM of CAIV), different concentrations of the tested compound, and 50 μM ANS or 200x diluted Glomelt™, in the 50 mM sodium phosphate buffer (at pH 7.0) containing 100 mM sodium chloride and 2–4% (v/v) of dimethylsulfoxide. To obtain the dissociation constant (at 37°C), the data analysis was performed, and the curves were fit using the Thermott web-server [14].

RESULTS AND DISCUSSION

Compound synthesis

In search of chemical compounds that exhibit a strong interaction with human CAIX, but a weakly interact with the remaining catalytically active human CA isozymes, we have designed and synthesised a series of fluorinated compounds shown in Scheme 1.

Compound **2** was synthesised using a sequential one-pot methodology. First, pentafluorobenzenesulfonamide **1** reacted with sodium benzenesulfinate, which gave an intermediate para substituted product – tetrafluoro-4-(phenylsulfonyl)benzenesulfonamide, that was not chromatographically purified. Instead, it was further reacted with ethylenediamine in the presence of triethylamine in DMSO at elevated temperature, yielding the desired product – 6,7-difluoro-8-(phenylsulfonyl)-1,2,3,4-tetrahydroquinoxaline-5-sulfonamide **(2)**. Compound **3** was synthesised by the *ortho* position substitution with benzylamine in a nonpolar solvent according to our already published methodology [15]. In the next stage, compound **3** was reacted with sodium benzenesulfinate, resulting in disubstituted 2-(benzylamino)-trifluoro-4-(phenylsulfonyl)benzenesulfonamide **(4)**. To see if it is possible to reduce the number of stages and chromatographic purifications, we again performed a one-pot reaction in the synthesis of compound **5**, where unlike in the synthesis of compound **4**, the intermediate *ortho* substituted 2-(cyclohexylamino)-tetrafluorobenzenesulfonamide was not chromatographically purified for

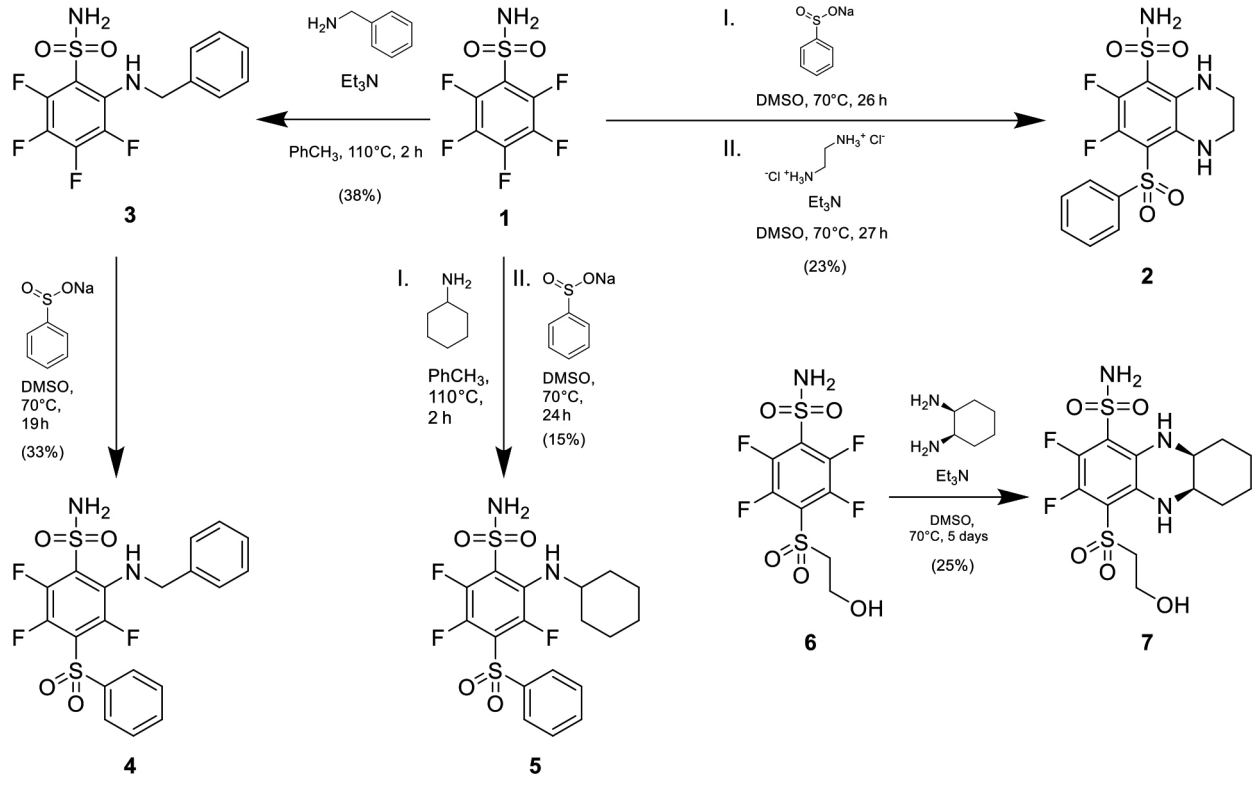

Scheme 1. Synthesis of compounds **2**, **3**, **4**, **5** and **7**

the next step of the reaction. Pentafluorobenzenesulfonamide **1** was first reacted with amino cyclohexane in toluene, to substitute the *ortho* position fluorine with an aminocyclohexane fragment. Then after changing the solvent, sodium benzenesulfonamide was introduced to turn the *ortho* substituted intermediate into the desired product **5**. Compound **7** was synthesised from **6** [12] using the same strategy as in the synthesis of compound **2**, but in this case using a different nucleophile – cis-1,2-diaminocyclohexane.

Compound binding to CA isozymes

The affinities of synthesised compounds were determined toward the selected human recombinant CA isozymes. In our opinion, the most robust assay providing the most accurate binding constants is the fluorescence-based thermal shift assay, also termed the differential scanning fluorimetry (FTSA, DSF). Figure 1 shows the thermal melting profiles and the dosing curves that yield the dissociation constant (K_d). Globular proteins, such as CA isozyme catalytic domains, unfold and denature upon heating, and the fluorescence of solvatochromic dyes used in the assay significantly increases. The midpoint of the increase corresponds to the melting temperature at which 50% of the protein is unfolded. Afterward, the fluorescence tends to decrease due to a general rule of decreasing fluorescence upon increasing temperature. The peak of maximal fluorescence is actually irrelevant for the assay. A ligand shifts this melting temperature toward a higher value. Note that there is no 'saturating' concentration. Continued increase of the compound concentration above the protein concentration threshold keeps pushing the T_m upwards. Resultant T_m datapoints are plotted against the logarithm of the ligand concentration and then fitted to a thermodynamic model, yielding the dissociation constant (K_d) and the enthalpies and heat capacities of the protein unfolding and binding processes. Thus, quite significant information is obtained about the protein stability and binding thermodynamics.

Calculation of the *Intrinsic* binding parameters

To calculate the intrinsic dissociation constant, we calculate the fractions of binding-ready sulfonamide and CA isozyme at pH 7.0 from the experimentally measured pK_a values. The fractions of the deprotonated inhibitor and the Zn-bound

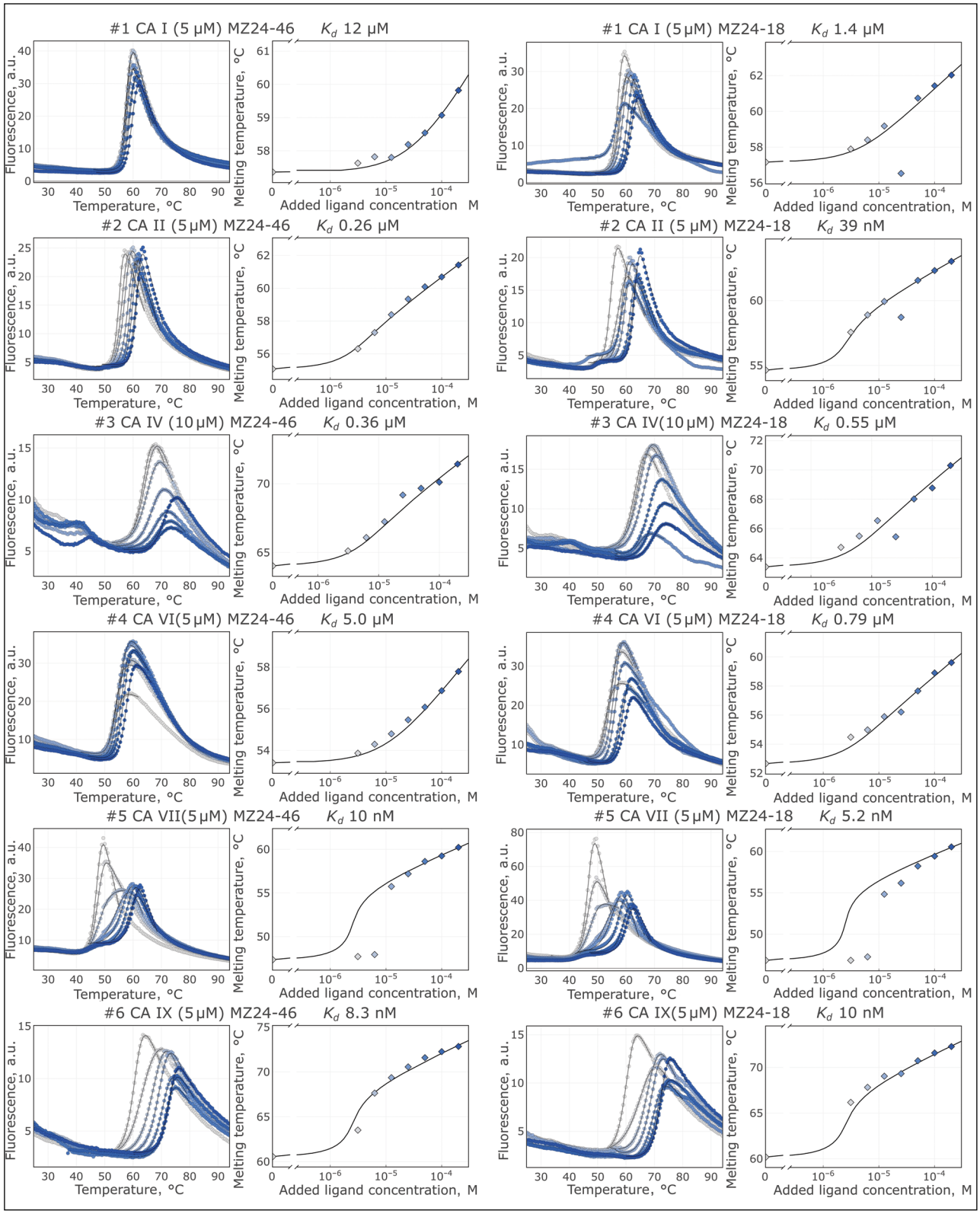

Fig. 1. Thermal shift assay profiles (FTSA) show examples of the determination of the observed dissociation constants. The left column shows compound **2** binding, while the right column shows that of compound **7**. The seven rows represent determinations for each CA isozyme in the order of increasing isozyme number. Two panels describe each interaction: raw fluorescence curves on the left show the determination of the melting temperature at each added compound concentration, while the resultant T_m values as a function of compound concentration are shown on the right panel. The fitted curve yielded K_d. The procedure was performed using the Thermott web server

Fig. 1. (Continued)

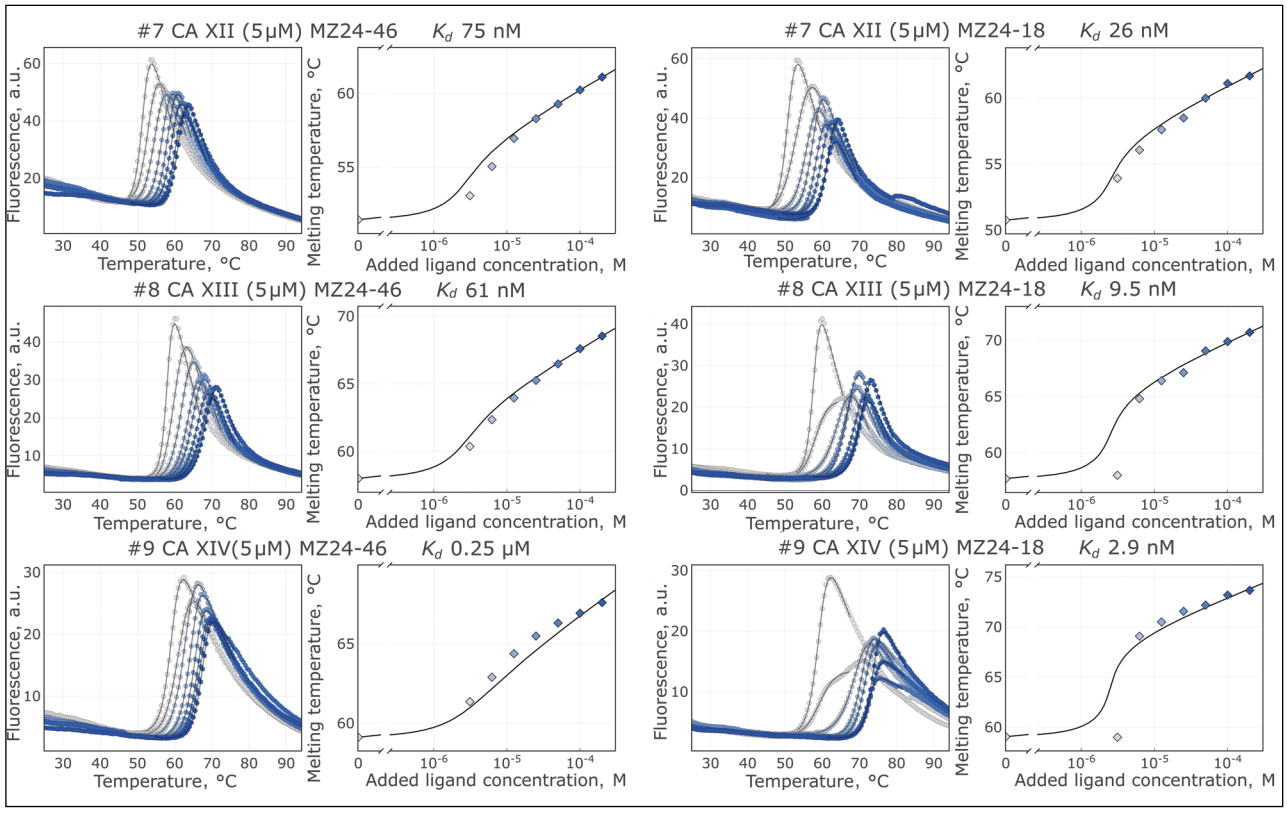

water form of CA can be calculated if both pK_a values are known (Eqs. (1, 2)):

$$f_{RSO_2NH^-} = \frac{10^{pH\text{-}pK_{a\_sulf}}}{1+10^{pH\text{-}pK_{a\_sulf}}}, \quad (1)$$

$$f_{CAZnH_2O} = 1 - \frac{10^{pH\text{-}pK_{a\_CAZnH_2O}}}{1+10^{pH\text{-}pK_{a\_CAZnH_2O}}}. \quad (2)$$

The pK_a values of the CA isozyme Zn-bound water molecules have been previously determined and explained in detail [16].

The pK_a of sulfonamide dissociation was determined by measuring UV–VIS absorbance spectra of the compound aqueous solution in buffers of various pH, usually in the range from 5 to 10, as previously described [17]. We took absorbance ratios approximately 10 nM below and above the isosbestic point, normalised the data and plotted them as a function of pH. Fitting of those curves yielded the sulfonamide pK_a of each compound.

The intrinsic dissociation constant $K_{d,\,int}$ is equal to the observed dissociation constant $K_{d,\,obs}$ multiplied by the fractions of a deprotonated inhibitor and a protonated Zn-bound water form of CA (Eq. 3):

$$K_{d,\,int} = K_{d,\,obs} \times f_{RSO_2NH^-} f_{CAZnH_2O}. \quad (3)$$

The affinities of synthesised compounds for nine human recombinant CA isozymes, determined by the FTSA, are listed in Table 1. These values represent the dissociation constants observed under experimental conditions. The only value that went into the picomolar range was the interaction between compound **5** and CAIX isozyme. It was equal to 0.33 nM. Possessing such high affinity, the compound also exhibited a quite significant selectivity since other isozymes bound much more weakly than CAIX, CAVII bound with 7 nM, while CAXII bound with 9 nM. Other isozymes bound even more weakly, especially the abundant CAI, which bound compound **5** with 5 μM (or 5000 nM) K_d. If we expect the working concentration of a compound in a biological setting to be in the order of 10 nM, it would nearly completely inhibit the cancer-associated CAIX, while affecting some 50% of CAVII, CAXII and CAXIII, and a little or negligible effect on the remaining tested isozymes.

Comparing the structures of synthesised compounds, compound **5** possesses the stiff *para-substituent* and a short *ortho-substituent*. The *ortho* substituent is necessary for the selectivity for

Table 1. **The observed dissociation constants ($K_{d, obs}$), in nM units, determined by the fluorescence-based thermal shift assay (FTSA), of synthesised compounds to selected human recombinant CA isozymes. The CAIII, CAVA and CAVB were not tested in this study. The dissociation constants are for 37°C and pH 7.0. Standard deviations of the values are within two-fold of the value**

Compound	CAI	CAII	CAIV	CAVI	CAVII	CAIX	CAXII	CAXIII	CAXIV
1, VD10-9 [16]	3.3	46	740	430	56	150	780	76	35
2, MZ24-18	14000	39	550	790	5.2	10	26	9.5	2.9
3, MZ24-21	350	390	ND	ND	14	25	380	ND	ND
4, MZ24-24	3500	370	2800	590	15	2.9	160	2.1	85
5, MZ24-3	5000	50	170	400	7.0	0.33	8.5	17	ND
6, VD10-35 [16]	0.20	17	510	67	7.1	41	250	29	33
7, MZ24-46	120000	260	360	5000	10	8.3	75	61	42
8, VD11-4-2 [16]	830	56	61	67	8.6	0.032	2.9	4	4.3
AZM	2400	46	86	220	13	21	130	79	63

CAIX. A more flexible, longer substituent in compound **4** showed a significantly weaker affinity for CAIX, most likely due to steric hindrance leading to a non-optimal position of the inhibitor. None of the synthesised inhibitors reached the affinity of a previously described compound, VD11-4-2 [8].

Intrinsic binding parameters

The experimentally determined binding affinities in the CA isozyme–sulfonamide compound system undergo two binding-linked protonation reactions. First, the Zn-bound electrostatically negative hydroxide protonates into a neutral water molecule, and, second, the neutral sulfonamide amino group deprotonates into a negatively charged anionic NH^- form. Both of these reactions significantly contribute to each thermodynamic parameter of binding and diminish the observed binding affinity. However, we are interested in the *intrinsic* affinity that would be observed if no such protonation reactions occurred. Thus, we must calculate these affinities, and only these affinities can be used in the rational drug design, where contributions of each functional group of the compound may be estimated.

The pK_a values of the CA isozyme Zn-bound water molecules have been previously determined by combining the thermal shift assay and isothermal titration calorimetry, and have been explained in detail previously [16]. Thus, these values were known and did not need to be determined again. However, we determined the pK_a of sulfonamide dissociation into an anionic form by measuring UV–VIS absorbance spectra of the compound aqueous solution in buffers of various pH, as previously described [17]. An example of such spectra is shown in Fig. 2a, for compound **7**. Upon deprotonation, the spectrum shifted to the lower wavelength, exhibiting an isosbestic point. We took absorbance ratios approximately 10 nM below and above the isosbestic point, normalised the data, and plotted them as a function of pH (Fig. 2b). Fitting of those curves yielded the pK_a of each compound.

The observed CA-ligand dissociation constant ($K_{d, obs}$) depends on the buffer pH due to diminishing fractions of the binding-ready components. Therefore, the affinity constant is distorted by the linked protonation reactions, and it is necessary to subtract their contribution. The calculated intrinsic dissociation constants ($K_{d, int}$) are listed in Table 2. The intrinsic dissociation constants are always lower than the values that we experimentally observe by any technique, since the linked protonation reactions always weaken the binding.

We can compare the gains or losses in affinity and selectivity observed upon chemical changes to the compound structure. First, we calculated the standard Gibbs energies of binding from $K_{d, int}$, and listed them next to the chemical structures shown in Fig. 3. The more negative the number, the tighter the association. Let us begin with compound **1** in the centre of the figure. This compound binds to CAI with the Gibbs energy of –57.4 kJ/mol. Compound **3**, to the left of compound **1**, bound to CAI with ΔG of –47.0 kJ/mol. Thus, the difference between **1** and **3** was 10.4 kJ/mol. The number is positive, thus **1** binds more weakly to CAI than **3**.

If we search for compounds with the strongest affinity for a particular CA isozyme, say CAIX, the previously described compound **8** (**VD11-4-2)** [8] binds to CAIX most strongly with a Gibbs energy

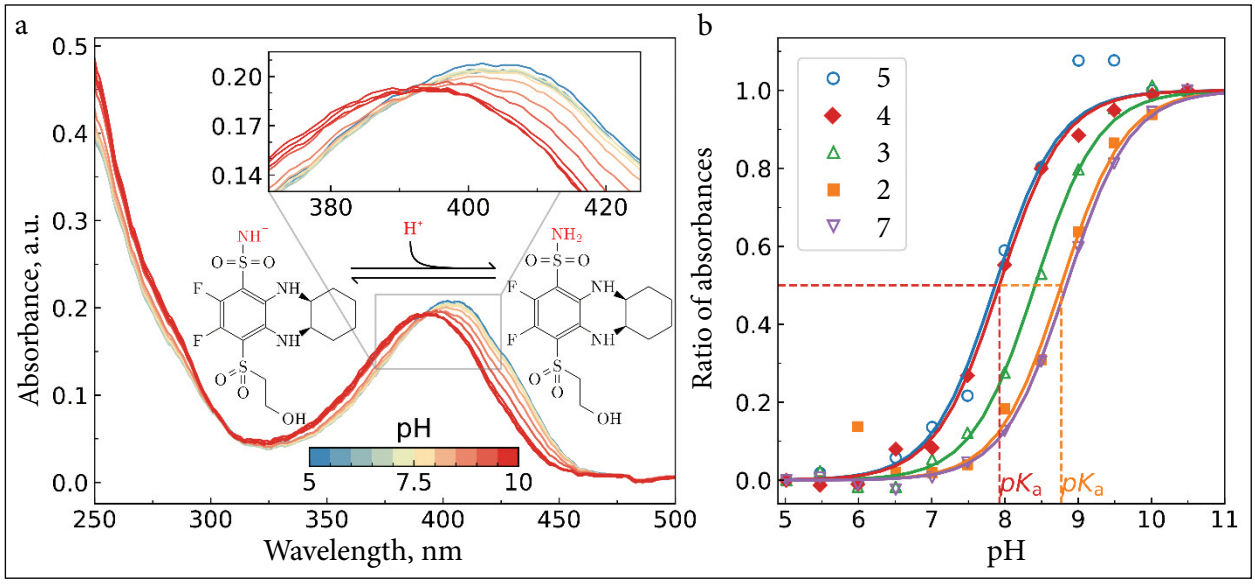

Fig. 2. Determination of the sulfonamide amino group pK_a by measuring the UV–VIS absorbance spectra of the compound aqueous solution in buffers of variable pH in the range from 5 to 10. Panel a shows the absorbance spectra, and panel b shows the normalised ratios of absorbances 10 nm below and above the isosbestic point of the spectra. Fitted curves yielded the pK_a of sulfonamide compounds

of –71.8 kJ/mol. However, we also need to consider the selectivity of binding, which is the difference in affinities for other isozymes. Compound **5** exhibits a strong affinity of –65.0 kJ/mol for CAIX and weaker affinities for all other CA isozymes than **8**. Sometimes it is not the main task to reach as high an affinity as possible, but, instead, it may be more important to seek selectivity that enables the compound to bind to the target and less to the off-target isozymes.

Carbonic anhydrase (CA) has been a classical model protein in studies of protein denaturation [19], folding [20], enzymatic activity [21], its inhibition [22] and protein interactions with small-molecule inhibitors [23] by various biophysical techniques. However, despite numerous studies and books devoted solely to the CA enzyme [24–29], and a model protein, it is still difficult to correctly predict and rationally design compounds that would distinguish among structurally closely related human CA isozymes and interact with a high affinity for only one of them. Therefore, the search for desired inhibitors and understanding of the mechanism of recognition remain important subjects in molecular biophysics and drug design.

As shown in our previous work, para-substituted benzenesulfonamides, such as **6** (*VD10-35*), exhibit the highest binding affinity for CAI [12]. However, if the *ortho* position on the pentafluorobenzenesulfonamide ring is substituted with an amine fragment, like in compound **3**, the trend is reversed. The binding affinity to CAI is reduced by four orders of magnitude (**3** CAI K_{d_int} – 12 nM, **6** CAI K_{d_int} – 0.064 nM), while the binding affinity to CAIX changes by only one order (**3** CAIX K_{d_int} – 0.27 nM, **6** CAIX K_{d_int} – 4.0 nM). This is explained by the interaction of the *ortho* position substituent with the hydrophobic pocket in the CAIX active site [8]. This interaction is one of the main factors in determining selectivity for the CAIX isozyme.

By adding a phenylsulfonyl fragment to such a compound into the *para* position (**4**), it is possible to achieve even higher binding affinity to CAIX and further decrease of the affinity to CAI. The affinity for CAIX increases by one order (**4** CAIX K_{d_int} – 0.088 nM, **3** CAIX K_{d_int} – 0.27 nM), while the affinity for CAI decreases by the same margin (**4** CAI K_{d_int} – 350 nM, **3** CAI K_{d_int} – 12 nM). If we exchange the benzylamine fragment in **4** with a cyclohexylamine fragment in **5**, the binding affinity to CAIX increases by one order of magnitude (**5** CAIX K_{d_int} – 0.011 nM). This can be explained by the flexibility of the cyclohexane ring, which might be needed for a more favourable interaction with the pocket, compared to a rigid benzylamine fragment.

The fact that benzylamine has an additional methylene linking group could also play a role

Table 2. **The intrinsic dissociation constants ($K_{d, int}$), in nM units, calculated from the observed affinities, determined by FTSA. Standard deviations of the $K_{d,int}$ values are within threefold of the value. The dissociation constants are for 37°C and valid for any pH. The first horizontal row below the names of the isozymes lists the pK_a values of the protein Zn-bound water molecule. The second green-shaded row lists the calculated fractions (*f*) of the binding-ready isozyme bearing the Zn-bound water molecule (not hydroxide anion). The second column, next to compound numbers, lists the pK_a of the compound sulfonamide group. Next column, shaded green, lists the fraction (*f*) of the binding-ready negatively charged sulfonamide group. Standard deviation of the pK_a groups is less than ±0.15 pH units. ND is not determined**

Compound			CAI	CAII	CAIV	CAVI	CAVII	CAIX	CAXII	CAXIII	CAXIV
			pK_a 8.1	6.9	6.6	6.0	6.8	6.6	6.8	8.0	6.8
Name	pK_a	*f*(SA^-)	*f*(CA) 0.93	0.44	0.29	0.09	0.39	0.29	0.39	0.91	0.38
			$K_{d, int}$, nM								
1	8.1	0.071	0.22	1.4	15	2.8	1.5	3.0	21	4.9	0.95
2	8.8	0.017	220	0.29	2.6	1.2	0.034	0.048	0.17	0.15	0.019
3	8.4	0.037	12	6.5	ND	ND	0.20	0.27	5.5	ND	ND
4	7.9	0.11	350	17	85	5.8	0.62	0.088	6.6	0.20	3.5
5	7.9	0.12	560	2.7	5.8	4.4	0.33	0.011	0.40	1.9	ND
6	7.3	0.34	0.064	2.6	50	2.1	0.95	4.0	33	9.1	4.4
7	8.8	0.014	1600	1.6	1.5	6.5	0.055	0.034	0.41	0.79	0.23
8	8.0	0.089	68	2.2	1.5	0.54	0.30	0.00081	0.10	0.32	0.15
AZM	7.0	0.50	1100	10	12	10	2.5	3.0	25	36	12

in determining the conformational energetics of the interaction. This is further examined in compounds **2** and **7**. Compound **2** does not possess a hydrophobic fragment, but contains a rigidified ethylene diamino fragment bound to the *ortho* and *meta* positions of the benzenesulfonamide ring. In contrast, **7** has a diamino cyclohexane fragment bound to the ring via two bonds as in **2**. Compound **2** bound weakly to CAI, K_{d_int} – 220 nM, but strongly to CAIX, K_{d_int} – 0.048 nM. It also moderately binds to other isozymes, though less to CAIV and CAVI. On the other hand, **7** exhibited even higher selectivity for CAIX over CAI (50000-fold) but retained binding affinity to CAIX in the same range as **2** and **4**.

In protein–ligand binding studies, as in any other research field, the issue of data accuracy and precision is of high importance. The binding studies involving proteins are sensitive to various factors, including solution pH, salt composition and concentration, the presence of additives such as buffer components, temperature, and other related factors. A slight variation in conditions may significantly affect the binding data. Recombinant proteins must be evaluated and validated to ensure their structural stability and enzymatic activity. It is important to repeat the experiments under the same conditions, yielding the standard deviation and increasing data precision.

However, we are not after the precision of a single technique, but would like to achieve accuracy. This can be done only by applying at least several orthogonal assays to measure the same protein–ligand interaction. For example, the affinity of a ligand for a protein could be determined by a stopped-flow assay of measuring the inhibition of enzymatic activity. This is the most common approach to measure compound binding to CA. However, this technique has a significant limitation since it cannot determine affinities below the used protein concentration, usually around 10–100 nM [30]. We have demonstrated that picomolar affinities cannot be determined by the SFA assay [31].

In high-affinity interaction measurements, we rely on the fluorescence-based thermal shift assay (TSA, FTSA), where the protein solution is heated, and the melting temperature is measured as a function of added ligand concentration. From this dependence, we calculate K_d and also obtain the enthalpies and heat capacities of protein unfolding and ligand binding. This technique, in our opinion, is best and can measure K_d values in the range from picomolar to millimolar in a single experiment [32]. This heating approach may be used by following the fluorescence or performing a differential scanning calorimetry (DSC) experiment [33]. However, despite the development of

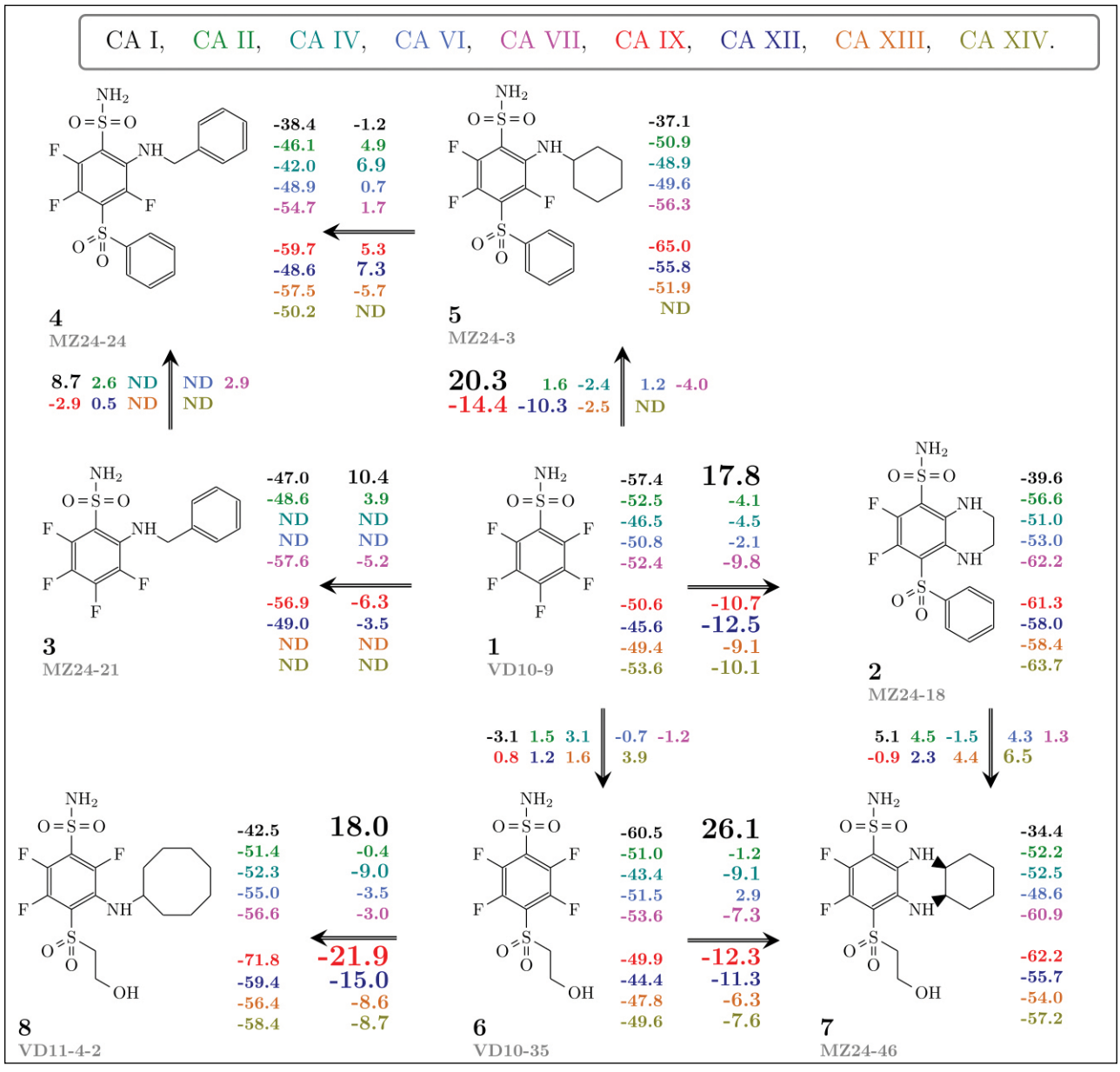

Fig. 3. Map of the correlation between compound chemical structures and intrinsic binding Gibbs energies to selected recombinant human CA isozymes. The numbers on the right of each structure list the standard intrinsic Gibbs energies of binding to each CA isozyme. The colours of each CA isozyme are shown at the top of the figure. The numbers above and below the arrows show the differences between adjacent, structurally closely related, chemical compounds. Larger changes are listed in a bigger font. The synthesis of compounds **1**, **6** and **8** has been described previously [8, 18].

the TSA (DSF, ThermoFluor) technique [34, 35] in the 1990s, it is still rather underused, primarily due to complex equations needed to determine affinity from the melting temperatures. To help here, we have made a web-server, Thermott, that will fit the T_m dependence on ligand concentration and estimate K_d for many ligands binding to globular proteins [36, 37].

Even if we determine K_d by numerous techniques and obtain the same value, the 'true' affinity of the sulfonamide compounds for CA isozymes is significantly different. This is because upon sulfonamide binding to CA, both the ligand and the protein undergo a binding-linked protonation reaction that consumes energy and reduces the *observed* affinity. We must account for the linked protonation reactions and obtain the *intrinsic* affinity. The intrinsic affinity is independent of pH, while the observed affinity is weaker both in the acidic and alkaline pH ranges for all 12 human CA isozymes [16, 38]. Only the intrinsic thermodynamic parameters correctly account for the structure-affinity relationships in

a structure-based drug design. We have tried and show the applications of this approach in the design of high-affinity compounds for CAIX [39].

The data for 600 synthetic compounds observed and intrinsic thermodynamic and kinetic parameters of binding to all 12 human catalytically active CA isozymes (8000 interaction measurements), together with 150 X-ray crystallographic structures, were assembled in the Protein–Ligand Binding Database (plbd.org) [3] for researchers to apply AI principles and use them for a more rational drug design. Unfortunately, no other laboratory currently reports intrinsic thermodynamics of compounds binding to CA, even though the binding-linked protonation reactions have been shown some time ago, and the principles have been put together for application toward rational drug design [6, 40, 41].

CONCLUSIONS

Several compounds were synthesised that possess a high affinity for cancer-associated CAIX, while a weakly binding to other CA isozymes, thus showing a high selectivity. Compound **5**, despite a slightly lower affinity for CAIX than the previous lead compounds, exhibited a higher selectivity over the remaining CA isozymes.

ABBREVIATIONS

AZM – acetazolamide
CA – carbonic anhydrase
CAI – carbonic anhydrase isozyme I
CAIX – carbonic anhydrase isozyme IX
DMF – dimethylformamide
DMSO – dimethyl sulfoxide
FTSA – fluorescence-based thermal shift assay
ND – not determined
NMR – nuclear magnetic resonance
TLC – thin layer chromatography
TSA – thermal shift assay

Received 20 October 2025
Accepted 5 December 2025

References

1. G. Klebe, *Drug Design: From Structure and Mode-of-action to Rational Design Concepts*, Springer Berlin Heidelberg, Berlin, Heidelberg (2024) [https://doi.org/10.1007/978-3-662-68998-1].
2. M. Puleva, L. Medrano Sandonas, B. D. Lörincz, et al., *Nat. Commun.*, **16(1)**, 8583 (2025) [https://doi.org/10.1038/s41467-025-63587-9].
3. D. Lingė, M. Gedgaudas, A. Merkys, et al., *Database*, 2023, baad040 (2023) [https://doi.org/10.1093/database/baad040].
4. A. Petrosiute, A. Zakšauskas, V. Lučiūnaitė, et al., *Br. J. Pharmacol.*, **182(7)**, 1610 (2025) [https://doi.org/10.1111/bph.17429].
5. K. D'Ambrosio, A. Di Fiore, V. Alterio, et al., *Chem. Rev.*, **125(1)**, 150 (2025) [https://doi.org/10.1021/acs.chemrev.4c00278].
6. V. M. Krishnamurthy, G. K. Kaufman, A. R. Urbach, et al., *Chem Rev*, **108(3)**, 946 (2008) [https://doi.org/10.1021/cr050262p].
7. J. Brynda, P. Mader, V. Sicha, et al., *Angew Chem. Int. Ed. Engl.*, **52(51)**, 13760 (2013) [https://doi.org/10.1002/anie.201307583].
8. V. Dudutienė, J. Matulienė, A. Smirnov, et al., *J. Med. Chem.*, **57(22)**, 9435 (2014) [https://doi.org/10.1021/jm501003k].
9. A. Vaškevičius, M. Žvirblis, M. Kurtenoka, et al., *J. Med. Chem.* (2025) [https://doi.org/10.1021/acs.jmedchem.5c01142].
10. A. Vaškevičius, D. Baronas, J. Leitans, et al., *eLife*, **13**, RP101401 (2024) [https://doi.org/10.7554/eLife.101401].
11. A. Zubrienė, V. Linkuvienė, D. Matulis, *Carbonic Anhydrase as Drug Target: Thermodynamics and Structure of Inhibitor Binding*, ed. D. Matulis, Springer International Publishing, Cham, 233 (2019) [https://doi.org/10.1007/978-3-030-12780-0_16].
12. V. Dudutienė, A. Zubrienė, A. Smirnov, et al., *Bioorg. Med. Chem.*, **21(7)**, 2093 (2013) [https://doi.org/10.1016/j.bmc.2013.01.008].
13. R. A. Copeland, *Evaluation of Enzyme Inhibitors in Drug Discovery: A Guide for Medicinal Chemists and Pharmacologists*, John Wiley & Sons (2013).
14. M. Gedgaudas, D. Baronas, E. Kazlauskas, V. Petrauskas, D. Matulis, *Drug Discov. Today*, **27(8),** 2076 (2022) [https://doi.org/10.1016/j.drudis.2022.05.008].
15. V. Dudutienė, A. Zubrienė, A. Smirnov, et al., *Chem Med Chem.*, **10(4)**, 662 (2015) [https://doi.org/10.1002/cmdc.201402490].
16. V. Linkuvienė, A. Zubrienė, E. Manakova, et al., *Q. Rev. Biophys.*, **51**, 1 (2018) [https://doi.org/10.1017/S0033583518000082].
17. P. W. Snyder, J. Mecinović, D. T. Moustakas, et al., *Proc. Natl. Acad. Sci. U. S. A.*, **108(44)**, 17889 (2011) [https://doi.org/10.1073/pnas.1114107108].
18. A. Zubrienė, J. Smirnovienė, A. Smirnov, et al., *Biophys Chem.*, **205**, 51 (2015) [https://doi.org/10.1016/j.bpc.2015.05.009].

19. K.-P. Wong, C. Tanford, *J. Biol. Chem.*, **248(24)**, 8518 (1973) [https://doi.org/10/gkzn7h].
20. L. G. Martensson, B. H. Jonsson, P. O. Freskgard, A. Kihlgren, M. Svensson, U. Carlsson, *Biochemistry*, **32(1)**, 224 (1993).
21. J. A. Verpoorte, S. Mehta, J. T. Edsall, *J. Biol. Chem.*, **242(18)**, 4221 (1967) [https://doi.org/10.1016/s0021-9258(18)95800-x].
22. R. G. Khalifah, *J. Biol. Chem.*, **246(8)**, 2561 (1971).
23. D. G. Myszka, Y. N. Abdiche, F. Arisaka, et al., *J. Biomol. Technol.*, **14(4)**, 247 (2003).
24. S. J. Dodgson, R. E. Tashian, G. Gros, N. D. Carter (eds.), *The Carbonic Anhydrases*, Springer US, Boston, MA (1991) [https://doi.org/10.1007/978-1-4899-0750-9].
25. W. R. Chegwidden, N. D. Carter, Y. H. Edwards (eds.), *The Carbonic Anhydrases*, Birkhäuser Basel, Basel (2000) [https://doi.org/10.1007/978-3-0348-8446-4].
26. C. T. Supuran, A. Scozzafava, J. Conway, *Carbonic Anhydrase: Its Inhibitors and Activators*, CRC Press, 1 (2004).
27. S. C. Frost, R. McKenna (eds.), *Carbonic Anhydrase: Mechanism, Regulation, Links to Disease, and Industrial Applications*, Subcellular Biochemistry, Springer Netherlands, Dordrecht, 75 (2014) [https://doi.org/10.1007/978-94-007-7359-2].
28. D. Matulis, *Carbonic Anhydrase as Drug Target: Thermodynamics and Structure of Inhibitor Binding*, Springer Nature (2019).
29. W. R. Chegwidden, N. D. Carter (eds.), *The Carbonic Anhydrases: Current and Emerging Therapeutic Targets*, Progress in Drug Research, Springer International Publishing, Cham, 75 (2021) [https://doi.org/10.1007/978-3-030-79511-5].
30. R. A. Copeland, in: *Evaluation of Enzyme Inhibitors in Drug Discovery*, John Wiley & Sons, Ltd, 245 (2013) [https://doi.org/10.1002/9781118540398.ch7].
31. J. Smirnovienė, V. Smirnovas, D. Matulis, *Anal. Biochem.*, **522**, 61 (2017) [https://doi.org/10.1016/j.ab.2017.01.022].
32. V. Petrauskas, E. Kazlauskas, M. Gedgaudas, L. Baranauskienė, A. Zubrienė, D. Matulis, *TrAC Trends Anal. Chem.*, **170**, 117417 (2024) [https://doi.org/10.1016/j.trac.2023.117417].
33. V. Linkuvienė, A. Zubrienė, D. Matulis, *Biochim. Biophys. Acta BBA – Proteins Proteomics*, **1870(9)**, 140830 (2022) [https://doi.org/10.1016/j.bbapap.2022.140830].
34. D. Matulis, J. K. Kranz, F. R. Salemme, M. J. Todd, *Biochemistry*, **44(13)**, 5258 (2005) [https://doi.org/10.1021/bi048135v].
35. M. W. Pantoliano, E. C. Petrella, J. D. Kwasnoski, et al., *J. Biomol. Screen.*, **6(6)**, 429 (2001) [https://doi.org/10.1177/108705710100600609].
36. M. Gedgaudas, D. Baronas, E. Kazlauskas, V. Petrauskas, D. Matulis, *Drug Discov. Today*, **27(8)**, 2076 (2022) [https://doi.org/10.1016/j.drudis.2022.05.008].
37. J. P. L. Franco Cairo, T. L. R. Corrêa, W. A. Offen, et al., *Nat. Commun.*, **16(1)**, 9244 (2025) [https://doi.org/10.1038/s41467-025-64309-x].
38. A. Zubrienė, D. Matulis, in: D. Matulis (ed.), *Carbonic Anhydrase as Drug Target: Thermodynamics and Structure of Inhibitor Binding*, Springer International Publishing, Cham, 107 (2019) [https://doi.org/10.1007/978-3-030-12780-0_8].
39. V. Paketurytė-Latvė, A. Smirnov, E. Manakova, et al., *IUCrJ*, **11(4)**, 556 (2024) [https://doi.org/10.1107/S2052252524004627].
40. P. W. Taylor, R. W. King, A. S. V. Burgen, *Biochemistry*, **9(20)**, 3894 (1970) [https://doi.org/10.1021/bi00822a007].
41. B. M. Baker, K. P. Murphy, *Biophys. J.*, **71(4)**, 2049 (1996) [https://doi.org/10.1016/S0006-3495(96)79403-1].

Mantas Žvirblis, Vaida Paketurytė-Latvė, Marius Gedgaudas, Darius Lingė, Ernestas Urniežius, Tautvydas Kojis, Laimonas Stančaitis, Audrius Zakšauskas, Aurelija Mickevičiūtė, Jelena Jachno, Vaida Juozapaitienė, Virginija Dudutienė, Asta Zubrienė, Daumantas Matulis

ORTO-/META-PAKAITAIS MODIFIKUOTŲ SELEKTYVIŲ KARBOANHIDRAZĖS IX INHIBITORIŲ PROJEKTAVIMAS